AGU PUBLICATIONS

Geophysical Research Letters

RESEARCH LETTER
10.1002/2015GL064156

Key Points:
- Ocean circulation is partitioned into thermally direct and indirect components
- With anthropogenic warming, cooling due to the direct component ceases
- Deep warming is set by the strength of the mean thermally indirect circulation

Correspondence to:
J. D. Zika,
j.d.zika@soton.ac.uk

Citation:
Zika, J. D., F. Laliberté, L. R. Mudryk, W. P. Sijp, and A. J. G. Nurser (2015), Changes in ocean vertical heat transport with global warming, *Geophys. Res. Lett.*, *42*, 4940–4948, doi:10.1002/2015GL064156.

Received 9 APR 2015
Accepted 19 MAY 2015
Accepted article online 26 MAY 2015
Published online 29 JUN 2015

Changes in ocean vertical heat transport with global warming

Jan D. Zika[1], Frédéric Laliberté[2], Lawrence R. Mudryk[2], Willem P. Sijp[3], and A. J. G. Nurser[4]

[1]University of Southampton, National Oceanography Centre, Southampton, UK, [2]Department of Physics, University of Toronto, Toronto, Ontario, Canada, [3]Climate Change Research Centre, University of New South Wales, Kensington, New South Wales, Australia, [4]National Oceanography Centre, Southampton, UK

Abstract Heat transport between the surface and deep ocean strongly influences transient climate change. Mechanisms setting this transport are investigated using coupled climate models and by projecting ocean circulation into the temperature-depth diagram. In this diagram, a "cold cell" cools the deep ocean through the downwelling of Antarctic waters and upwelling of warmer waters and is balanced by warming due to a "warm cell," coincident with the interhemispheric overturning and previously linked to wind and haline forcing. With anthropogenic warming, the cold cell collapses while the warm cell continues to warm the deep ocean. Simulations with increasingly strong warm cells, set by their mean Southern Hemisphere winds, exhibit increasing deep-ocean warming in response to the same anthropogenic forcing. It is argued that the partition between components of the circulation which cool and warm the deep ocean in the preindustrial climate is a key determinant of ocean vertical heat transport with global warming.

1. Introduction

As the climate has warmed over the past decades, the ocean has absorbed more than 5 times as much heat as all other components of the Earth system combined [*Solomon et al.*, 2007] with significant consequences for global sea level rise [*Domingues et al.*, 2008]. Regardless of future greenhouse gas emissions, past warming of the ocean will influence global atmospheric temperatures into the foreseeable future [*Held et al.*, 2010].

A recent study by *Kuhlbrodt and Gregory* [2012] concluded that for a given surface warming, climate models exhibited a large spread in ocean heat uptake. Using data from the fifth Climate Model Intercomparison Project (CMIP5), they found some indication that the eddy-induced transport parameter influenced the differences in uptake efficiency among models. The eddy-induced transport parameter is thought to set the strength of the Southern Ocean overturning circulation given Southern Hemisphere winds and stratification [*Marshall and Radko*, 2003]. In addition, *Kostov et al.* [2014], also using CMIP5, found that the depth of penetration of Atlantic Meridional Overturning Circulation was a good indicator of ocean heat uptake efficiency. Both *Kuhlbrodt and Gregory* [2012] and *Kostov et al.* [2014] suggest that differences in deep-ocean circulation set differences in heat uptake efficiency between ocean models. However, it is unclear how to quantify this effect and how different components of the circulation set these differences.

Classical models draw a link between the mean circulation and vertical heat transport. *Munk* [1966] and *Stommel and Arons* [1960] related the downward heat transport by small-scale vertical mixing to an upward heat transport by a thermally direct overturning circulation. Such a circulation is known as thermally direct, because, like a heat engine, kinetic energy can be drawn from the upwelling of buoyant warm water and downwelling of dense cold water. Although the Antarctic bottom water circulation is still thought to be driven in such a way, *Toggweiler and Samuels* [1995] proposed that a pole to pole overturning circulation in the upper 2000 m could be set by Southern Hemisphere winds and hence would be thermally indirect. Numerous studies have since explored the link between the pole to pole and Antarctic bottom water circulations, vertical mixing, Southern Hemisphere winds, and the compensating effect of mesoscale eddies [*Gnanadesikan*, 1999; *Zhang and Vallis*, 2013; *Wolfe et al.*, 2008; *Shakespeare and Hogg*, 2012]. However, the link between this circulation and the vertical heat budget is seldom discussed—*Marshall and Zanna* [2014] and *Kostov et al.* [2014] being exceptions.

Water masses are warmer and more saline in the North Atlantic and cooler and less saline at the same density and depth in the Southern Ocean [*Marshall and Speer*, 2012]. Hence, if upwelling and downwelling occur at the same density, the pole to pole circulation can lead to a net downward flux of heat. This would imply a thermally indirect circulation (i.e., one that does not draw kinetic energy from the thermal stratification).

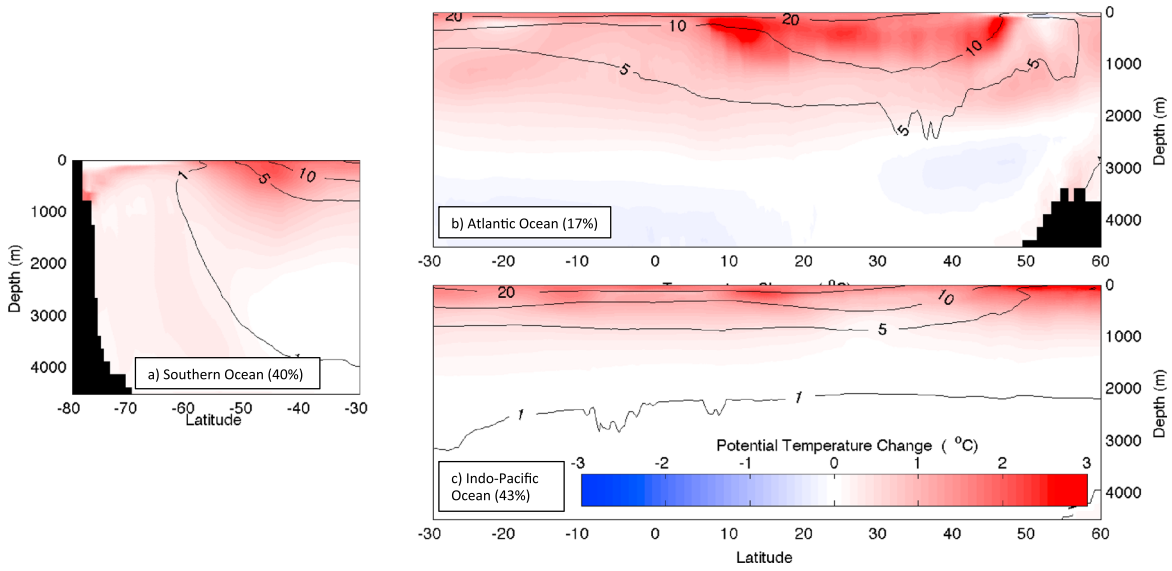

Figure 1. Zonally averaged preindustrial mean temperature (contours) and temperature change (color map) between 1850 and 2100 in the RCP4.5 scenario simulation of CCSM4 in degrees Celsius in (a) the Southern Ocean, (b) the Atlantic Ocean only, and (c) the Indian and Pacific Oceans. The contributions of each region to the total ocean heat content change are shown in brackets.

Gnanadesikan et al. [2005] and *Gregory* [2000] indeed find that resolved advection leads to downward flux of heat into the deep ocean in the upper 2000 m of coarse-resolution climate models. *Zika et al.* [2013a] proposed that the circulation could have two counteracting components: (i) a pole to pole overturning circulation fluxing heat downward and (ii) an Antarctic bottom water circulation fluxing heat upward.

Here we argue that the way transient heat uptake responds to a warming climate is informed by how different components of the circulation contribute to the mean vertical heat balance.

2. Results

2.1. Ocean Warming in a Climate Model

We analyze the output of the ocean component of the Community Climate System Model, version 4 (CCSM4) [*Gent et al.*, 2011] over two periods: an equilibrated preindustrial period (845–875 years after initialization from rest) and a transient climate simulation (1980–2100), using a combination of estimated historical emissions and Representative Concentration Pathway 4.5 (RCP4.5). See Appendix A for a complete description of the simulations used. Between the preindustrial state and 2100 the ocean warms by approximately 3°C at the surface and by 1°C at 1000 m depth. Warming is more pronounced in the North Atlantic (Figure 1b) as was found in previous studies [*Lee et al.*, 2011]. However, the Atlantic's contribution to the total warming is small due to its small volume relative to the Southern Ocean and the combined Pacific and Indian Oceans (Figure 1c).

In addition to a contrast in warming between the Atlantic and Indo-Pacific basins, there is a weak warming (less than 1°C) of the deep Southern Ocean that extends well below 2000 m. The preindustrial state has a small cooling drift associated with an upward heat transport which is less than 0.05 W m^{-2} (all heat fluxes are calculated in Watts and converted to W m^{-2} by dividing by the area of the earth) at all depths, in the global average. The cooling seen in the deep North Atlantic is a continuation of this drift.

2.2. The Thermal Circulation

Here we quantify the accumulated vertical transport of water masses (Ψ_T) in potential temperature (T) coordinates as

$$\Psi_T(T^*) = \int\int \Pi(T^* - T)\, w_{\text{res}}\, dxdy. \tag{1}$$

Here Π is a step function ($\Pi(T^* - T) = 0$ for $T^* - T < 0$ and 1 otherwise) and w_{res} is the residual vertical velocity. The residual velocity is the sum of the Eulerian and eddy-induced components of vertical advection (i.e., including advection due to the parameterizations for mesoscale eddies of *Gent and McWilliams* [1990] and

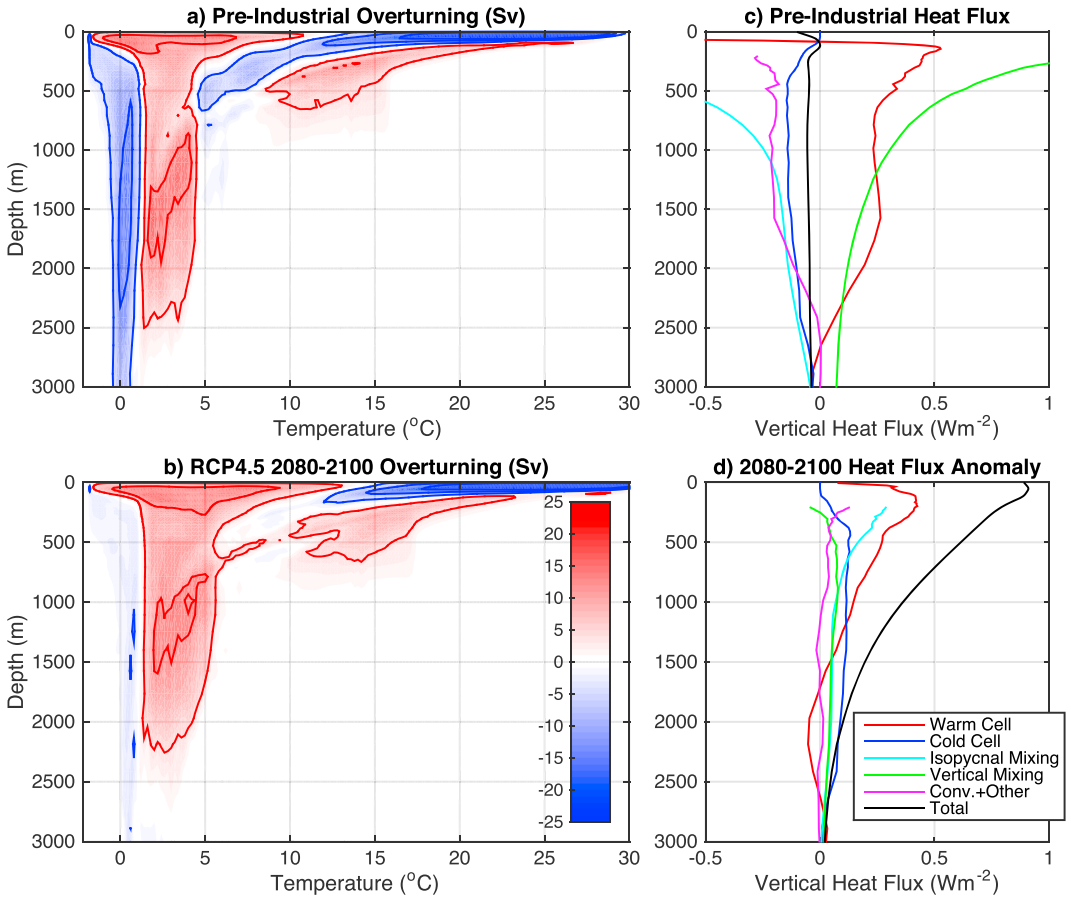

Figure 2. (a and b) Accumulated vertical volume transport in temperature coordinates at each depth level of CCSM4 including both the Eulerian and eddy-induced velocities in Sverdrup (Sv). Negative (blue) components circulate in an anticlockwise direction. Positive (red) components circulate in a clockwise direction. The cold cell, discussed in the text, is the blue anticlockwise cell that occupies water colder than 1°C. The warm cell is the red clockwise cell (we define the vertical heat transport due to the warm cell as including the anticlockwise cell at temperatures warmer than 4°C and shallower than 800 m). (c and d) Vertical heat flux due to the warm cell (red), the cold cell (blue), background vertical mixing (green), isopycnal mixing (magenta), the sum of all other contributions including parameterized convection (cyan), and the total (black). Shown are averages for years 845 to 875 of the preindustrial simulation (Figures 2a and 2c), the average for years 2080 to 2100 of the RCP4.5 scenario simulation (Figure 2b) and the difference between years 2080 and 2100 of the RCP4.5 scenario simulation and the preindustrial period (Figure 2d).

submesoscale processes of *Fox-Kemper et al.* [2008]). Here we use potential temperature as our heat variable as it is perfectly conserved in the numerical models considered. In an observational context, conservative temperature would be a more appropriate variable since it is more accurately conserved [*McDougall*, 2003].

The quantity Ψ_T has a number of useful properties:

1. As Ψ_T describes the upwelling and downwelling of waters at different temperatures, the vertical heat transport due to the resolved circulation can be diagnosed from it. In addition, the advective vertical heat transport can be attributed to distinct components of the circulation defined by closed contours of Ψ_T [*Ferrari and Ferreira*, 2011; *Zika et al.*, 2013b].
2. Where haline effects are small, Ψ_T can be interpreted in terms of the energetics of the resolved circulation. The quantity Ψ_T can be used to diagnose how much each component of the circulation lowers or raises the center of mass of the ocean and hence how much energy is transferred from potential to kinetic reservoirs [*Nycander et al.*, 2007].

It must be stressed that for the ocean circulation in a transient state (such as a global warming scenario) vertical exchanges of water masses can occur without corresponding deep-ocean water mass transformations. In such

a case, Ψ_T may not represent a "stream function" and is only used here to describe the vertical exchanges of waters at different temperatures.

We choose to use the depth-temperature overturning (Ψ_T) as our diagnostic here rather than the conventional meridional overturning circulation in depth-latitude or density-latitude coordinates because there is no direct link between the circulation defined in a meridional coordinate and the vertical heat transport. Covariations in the temperature and vertical velocity at constant latitude can be significant particularly the Southern Ocean [*Zika et al.*, 2013a].

We have computed Ψ_T from the sum of the Eulerian, parameterized mesoscale eddy, and submesoscale eddy-induced velocities for 30 years of monthly CCSM4 data (Figure 2a).

The accumulated transport in temperature coordinates for the preindustrial climate of CCSM4 (Figure 2a) displays the same thermally direct and thermally indirect cells described by *Zika et al.* [2013a]. The coldest cell involves downwelling of cold water and upwelling of warmer water. We will refer to this cell as the "cold cell" (anticlockwise blue cell on the left of Figure 2a). The warmer waters are associated with upwelling of cool water and downwelling of relatively warm water. This will be referred to as the "warm cell" (clockwise red cell in Figure 2a). *Zika et al.* [2013a] linked the cold cell geographically and by its water mass properties to Antarctic bottom water. The warm cell was linked geographically to the Southern Ocean and Atlantic Meridional Overturning Circulation. Southern Hemisphere winds have been found to be the source of energy maintaining the warm cell [*Saenko*, 2009; *Zika et al.*, 2013a]. The anticlockwise cell in the upper ocean and at temperatures warmer than 4°C was linked by *Zika et al.* [2013a] to the subtropical gyres and tropical circulation. Although the distinct contribution of those cells to the vertical heat transport may be of interest, the focus of this study is largely on the ocean below 800 m depth.

The vertical heat transport due to the cold and warm cells is quantified, after integrating by parts, as

$$H_{\text{cold}} = C_p \rho_0 \int_{T_{\min}}^{T_u} \Psi_T \, \mathrm{d}T, \tag{2}$$

$$H_{\text{warm}} = C_p \rho_0 \int_{T_u}^{T_{\max}} \Psi_T \, \mathrm{d}T, \tag{3}$$

where C_p is the heat capacity of seawater, ρ_0 is the average density, $T_u \approx 1$°C is the temperature separating the cold and warm cells such that $\Psi_T(T_u) = 0$, and $T_{\max}$ and $T_{\min}$ are the maximum and minimum ocean temperatures, respectively. In the above definition, heat transport by the warm cell includes the shallow cells warmer than 4°C and found above 800 m depth.

In the preindustrial state the warm cell gives a globally averaged downward heat flux of 0.22 W m^{-2} at 1000 m depth, whereas the cold cell fluxes 0.14 W m^{-2} of heat upward at the same depth (Figure 2c).

It is important to note that Ψ_T does not describe the vertical heat flux due to nonadvective subgrid-scale processes including small-scale turbulent mixing, isopycnal mixing, and parameterized convection. We diagnose the contributions to the vertical heat flux including the effect of background vertical mixing, isopycnal mixing, and the sum of the remaining processes including subgrid convection, the effect of the sampling frequency used, and variations in the state-dependent isopycnal mixing coefficient (Figure 2c; green, cyan, and magenta lines, respectively). How these components are diagnosed is detailed in Appendix B.

Background vertical mixing warms the deep ocean at a mean rate of 0.27 W m^{-2} at 1000 m in the preindustrial state, isopycnal mixing cools at a rate of 0.2 W m^{-2}, and the sum of convective and other remaining processes cools at 0.19 W m^{-2} (Figure 2b). These results are broadly consistent with previous analysis of other models [*Gregory*, 2000; *Morrison et al.*, 2013].

2.3. Response of the Depth-Temperature Overturning to Anthropogenic Warming

As the surface of the ocean warms under forcing from anthropogenic emissions, the thermal circulation responds in three distinct ways:

1. The warm cell maintains the same peak in transport at each depth level, but the difference in temperature between the upwelling and downwelling branches becomes larger (Figure 3b). This results in the cell fluxing more heat downward (Figure 3d).
2. The cold cell becomes both weaker and covers a smaller range of temperatures (Figure 3b). As a result, the cold cell is fluxing less heat upward (Figure 3b).

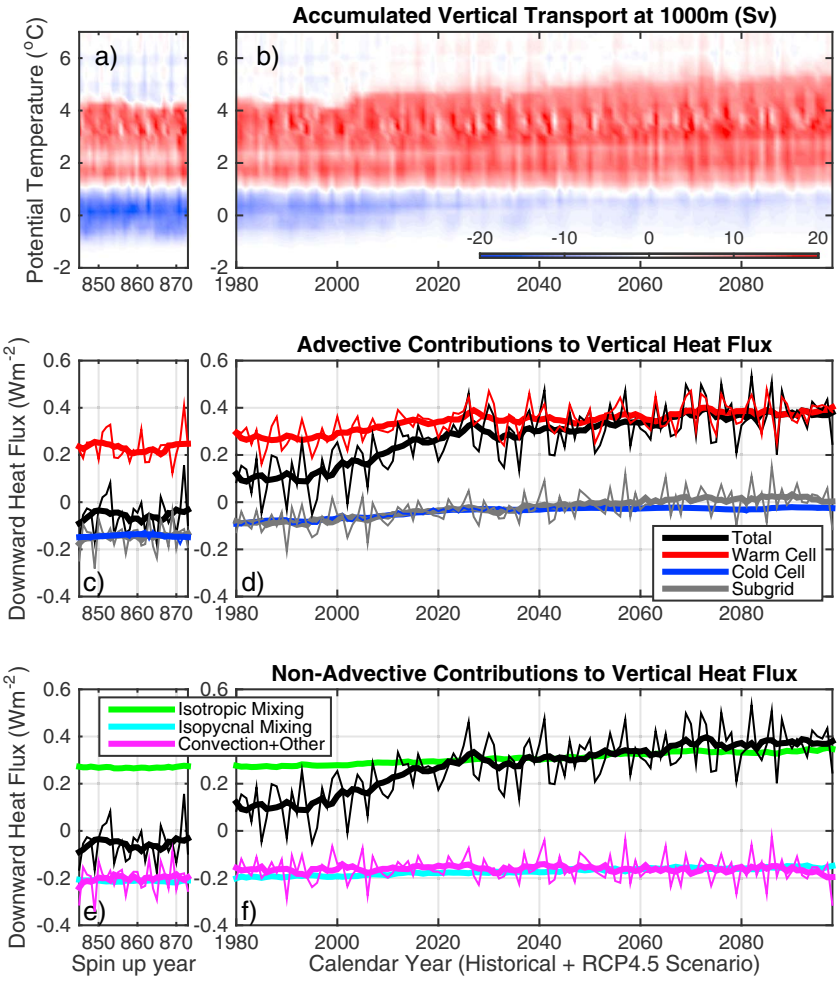

Figure 3. (a and b) Annual average accumulated vertical volume transport in temperature coordinates at 1000 m depth in CCSM4 in Sverdrup (Sv). (c and d) Contributions to the downward heat transport at 1000 m with the heat transport due to all processes (black), the warm cell (red), and the cold cell (blue). These are grouped as "advective" terms since they are due to the sum of the Eulerian and eddy-induced velocities in the model. (e and f) Vertical heat flux due to changes in the vertical temperature gradient (green), changes in the isopycnal temperature gradient (magenta), the sum of all other contributions including parameterized convection and the effect of changing isopycnal mixing coefficients (cyan), and the total (black). These are grouped as "nonadvective" terms since they are parameterized as diffusion rather than advection in the model. Shown are time series for the preindustrial climate simulation (Figures 3a, 3c, and 3e) and the historical and RCP4.5 scenario simulation (Figures 3b, 3d, and 3f).

3. Deep cooling due to subgrid-scale processes, largely isopycnal mixing, reduces, leading to warming of the deep ocean.

With anthropogenic warming the warm cell transports more heat downward. Concomitantly, the subgrid-scale fluxes and the cold cell heat transport are reduced, switching off almost completely at 1000 m depth by 2100 (Figures 2b and 3b). Because of the reduction in upward heat flux by the cold cell and non-advective processes (which were previously cooling the deep ocean; Figures 3c–3f), by 2060 the total heat transport at 1000 m approaches that of the warm cell (Figure 3d). As the vertical heat flux at 1000 m increases, there is some shoaling of the warm cell suggesting the downwelling branch does not penetrate as deeply (Figure 2c).

The relationship between the total vertical heat transport and the width of the warm cell is considered by multiplying the maximum of the preindustrial time mean Ψ_T at 1000 m ($\overline{\Psi}$) by the transport weighted difference in temperature between the upwelling and downwelling branches of the warm cell (ΔT), which evolves in time. The heat transport predicted by $C_p \rho_0 \overline{\Psi} \Delta T$ is plotted versus both the warm cell's true heat transport

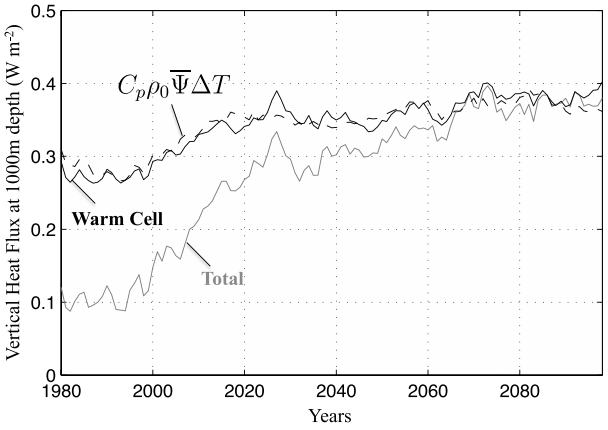

Figure 4. Ten year running mean vertical heat transport at 1000 m depth in CCSM4. Shown are the total (grey) that due to the warm cell (black solid) and predicted by the mean maximum stream function from the preindustrial state ($\overline{\Psi}$) multiplied by the running mean temperature difference within the cell (ΔT) (dashed).

and the total heat transport at 1000 m depth (Figure 4). The decadally averaged time series of the predicted heat flux differs from the actual heat flux by the warm cell by less than 5%.

Although the reduction in the strength of the cold cell could be interpreted in terms of a capping of a thermally driven circulation, the convective flux does not appear to respond in such a way. The convective heat flux (including residuals from the other mixing terms) at 1000 m depth does not vary considerably over the climate change simulation, decreasing modestly from 0.2 W m^{-2} to 0.19 W m^{-2} in the first half of the 21st century before recovering to 0.2 W m^{-2} by the 2080–2100 period (Figures 2d, 3e, and 3f). Instead, reduced deep cooling due to subgrid processes is accounted for by the change in the vertical temperature gradient between the warm and cold reservoirs on which vertical mixing and isopycnal mixing act. The combined change in heat flux represents a deep warming of 0.14 W m^{-2} (Figures 2d, 3e, and 3f).

3. Deep Warming by the Warm Cell in a Range of Climate Simulations

We now ask whether climate model simulations with stronger warm cells have larger vertical heat transport in their transient state. That is, is there a link between the strength of the mean circulation and how much heat the deep ocean takes up with global warming? Three experiments have been carried out with the Earth system model University of Victoria Intermediate Complexity Climate Model (UVIC) [*Weaver et al.*, 2001]. The simulations are named REF, TAU0.5, and TAU1.5 and are identical to those used by *Zika et al.* [2013a] (also see Appendix A for more details). The preindustrial states in the three models have different warm cells due to differing mean Southern Hemisphere wind forcing [*Zika et al.*, 2013a]. From the preindustrial states of these three models we instantaneously quadruple CO_2 concentrations to 4 times preindustrial levels.

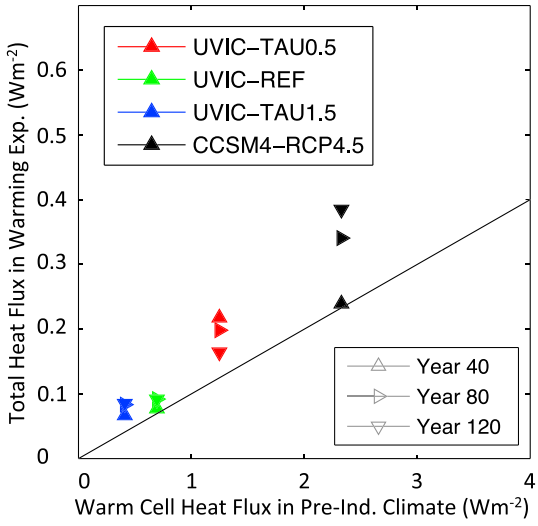

Figure 5. The vertical heat flux at 1000 m due to the warm cell in the preindustrial climate versus the total vertical flux in global warming experiments. Shown are the UVIC simulations: REF (green), TAU0.5 (blue), and TAU1.5 (red) where the three values for each model are the 40th (upward triangle), 80th (right triangle), and 120th (downward triangle) years since CO_2 was quadrupled. Also shown is the CCSM4 RCP4.5 simulation (black) for years 2020, 2060, and 2100 (upward, right, and downward triangles, respectively).

In each simulation, the cold cell weakens in response to greenhouse forcing. In REF the maximum transport of the cold cell at 1000 m depth reduces from 12.5 Sverdrup (Sv) in the preindustrial mean state to 4.5 Sv one century after CO_2 concentrations were quadrupled. Equivalent reductions were found for TAU0.5 and TAU1.5. Vertical heat transport due to the cold cell reduces proportionately to its maximum transport in each simulation. Meanwhile, the warm cell continues to warm the deep ocean at the same or at a faster rate. As in CCSM4, in each of the UVIC simulations the downward heat flux due to nonadvective subgrid processes increases with greenhouse warming although we did not investigate the role of each individual process.

In Figure 5, the total vertical heat transport at 1000 m for years 40, 80, and 120 of these experiments is compared to the warm cell heat transport in their respective preindustrial states (results from CCSM4 for years 2020, 2060, and 2100 of the RCP4.5 global warming scenario are also shown). Models with stronger warm cell heat transport in their preindustrial states have larger transient vertical heat transport in the initial century of our experiments. Our results are consistent with the hypothesis that deep cooling processes are reduced and deep advective warming process persists under global warming, although a larger and more diverse range of models is needed to infer a robust physical relationship.

4. Discussion and Conclusions

We have shown that the vertical heat transport in a state of the art climate model is related to a warm cell which fluxes heat downward and the combination of a cold cell and subgrid processes which flux heat upward. Under the RCP4.5 anthropogenic forcing scenario this system responds with a shutdown of the cold cell's cooling effect and an increase in the warm cell's warming effect.

Vertical heat transport sets ocean heat uptake efficiency and hence strongly influences transient climate change [*Gregory*, 2000]. Our results highlight the importance of ocean circulation, rather than ocean mixing, in setting this transfer, reaffirming the findings of *Marshall and Zanna* [2014]. Furthermore, we show that different parts of the circulation contribute differently to ocean heat uptake. Our finding that the interhemispheric overturning can passively downwell warm water leading to increased vertical heat transport is consistent with recent studies which found that both the Atlantic Meridional Overturning (the downwelling branch of the interhemispheric overturning) [*Kostov et al.*, 2014] and the coefficient for eddy-induced advection (a key regulator of the interhemispheric overturning) [*Kuhlbrodt and Gregory*, 2012] were linked to heat uptake efficiency. In addition, our finding that deep cooling is likely to reduce due to a slowdown in the Antarctic bottom water circulation is consistent with observed warming of regions of the ocean below 2000 m depth around Antarctica [*Purkey and Johnson*, 2010; *Wunsch and Heimbach*, 2014].

Our results suggest that in order to accurately predict transient ocean heat uptake, a climate model must accurately represent both the thermally direct and thermally indirect components of ocean circulation, their driving processes, and the parameterized processes which influence them. Furthermore, the link between the mean circulation and the resulting magnitude of global heat uptake suggests that an accurate representation of the mean state is paramount. This motivates future work developing ways of diagnosing the mean circulation from observations.

The simple description of the response of vertical advective heat transport to surface warming given in the previous sections comes with a number of important caveats. These include the following:

1. Deep cooling due to the cold cell may be strongly influenced by freshening and brine rejection by cryospheric processes which are not accounted for in our simple description of the ocean's response to warming.
2. Winds in the Southern Hemisphere could increase significantly, and eddy compensation could be muted in the real system, implying the transport could increase, increasing the heat transport due to the warm cell.
3. Mesoscale eddies are not explicitly resolved in the simulations discussed here.
4. Haline and regional processes could cause changes in the thermal circulation with warming, particularly in the North Atlantic. The AMOC is expected to weaken with surface warming and glacial melt, with an uncertain effect on Ψ_T.

Future work should investigate, for a range of models and climate states, the potential impact of these and other complications on this simple description of vertical heat exchange.

Appendix A: Numerical Model Experiments

The Community Climate System Model 4 (CCSM4) contains the Community Atmosphere Model 4, the Community Land Model 4, the Community Ice Code 4, and the Parallel Ocean Program 2 (see http://www.cesm.ucar.edu/ and *Gent et al.* [2011]). The atmosphere and land model are run on a nominally 2° finite volume grid, while the ocean and ice models are run on the nominally 1° Greenland dipole grid. The configuration is identical to the "coupled model" configuration described in *Mudryk et al.* [2013]. The model was initialized from the 500th year of the standard CCSM4 preindustrial (1850) control simulation (with 1° atmospheric resolution) and run for an additional 375 years with continued preindustrial forcing. From year 345 of

the control simulation, a second simulation was initialized, forced by time-dependent estimates of historical greenhouse gases, ozone, aerosols, volcanic emissions, and solar variability from 1850 to 2005. This second simulation was continued until 2100 using radiative forcing from the 4.5 W m^{-2} Representative Concentration Pathway (RCP4.5) [*Taylor et al.*, 2012].

CCSM4 has been widely validated in terms of its mean state and variability (see, for example, *Gent et al.* [2011] and the corresponding Journal of Climate Special Collection).

In CCSM4, an overflow parameterization involves advection where a topographic mask would typically exist. Upstream of sills, such as the Greenland-Scotland overflow region, advection is directed into the topography, and downstream of the sills, advection is directed out of the topography. In order to conserve the total volume of water, we include the advection due to the overflow parameterization in w_{res} and assume it occurs at the midpoint temperature and passes through all depth surfaces between the grid boxes upstream and downstream of the sill.

Anthropogenic warming experiments are conducted with the University of Victoria Intermediate Complexity Climate Model (UVIC) [*Weaver et al.*, 2001]. Configuration REF has winds set to present-day fields, while TAU0.5 (TAU1.5) has winds south of 30°S set to 50% less (more) than the present-day observations (configuration names are identical to those in *Zika et al.* [2013a]). After a 3000 year spin-up, the radiative forcing is perturbed, equivalent to an instant quadrupling of preindustrial CO_2 concentrations. UVIC uses a constant eddy mixing coefficient for tracers of 1200 m^2 s^{-1}.

Appendix B: Contributions to the Nonadvective Vertical Heat Flux

The vertical mixing contribution is estimated using the seasonal climatology of the vertical mixing coefficient (the sum of a background mean and that from a tidal mixing scheme) multiplied by the vertical temperature gradient. Likewise, the isopycnal contribution is the climatological mean isopycnal mixing coefficient (based on a three-dimensional state-dependent mixing scheme) multiplied by the vertical component of the temperature gradient projected onto a locally referenced neutral tangent plane [*Griffies*, 2007]. Since the small slope approximation is violated near the surface, we restrict these diagnostics to the ocean below 200 m. Tests carried out with interannually varying mixing coefficients for the preindustrial period differ from those using climatological coefficients by less than 10% below 200 m. The sensitivity above 200 m is significantly higher. Tests were also carried out interpolating horizontal gradients first onto the center of grid cells before projecting onto neutral tangent planes and after. The difference in vertical heat flux was again less than 10%. The remainder of the nonadvective heat flux is attributed to the sum of the convective parameterization and variations in vertical and isopycnal mixing coefficients with climate change.

Acknowledgments

J.Z. and A.G. acknowledge the support of the Natural Environment Research Council through grant NE/K012932/1 and National Capability Funding. W.S. acknowledges the support of the Australian Research Council through grant DP1096144. We thank Arnaud Czaja, Laure Zanna, and Andrew Hogg for their helpful feedback. Computations were performed on the TCS supercomputer at the SciNet HPC Consortium funded by the Canada Foundation for Innovation under the auspices of Compute Canada, the Government of Ontario, Ontario Research Fund Research Excellence, and the University of Toronto. The numerical model output and numerical model code used in this study can be made available to interested parties.

The Editor thanks Laure Zanna and Andrew Hogg for their assistance in evaluating this paper.

References

Domingues, C. M., J. A. Church, N. J. White, P. J. Gleckler, S. E. Wijffels, P. M. Barker, and J. R. Dunn (2008), Improved estimates of upper-ocean warming and multi-decadal sea-level rise, *Nature*, *453*, 1090–1093.

Ferrari, R., and D. Ferreira (2011), What processes drive the ocean heat transport, *Ocean Model.*, *38*, 171–186.

Fox-Kemper, B., R. Ferrari, and R. Hallberg (2008), Parameterization of Mixed Layer Eddies. Part I: Theory and diagnosis, *J. Phys. Oceanogr.*, *38*, 1145–1165.

Gent, P. R., and J. C. McWilliams (1990), Isopycnal mixing in ocean circulation models, *J. Phys. Oceanogr.*, *20*, 150–155.

Gent, P. R., et al. (2011), The Community Climate System Model version 4, *J. Clim.*, *24*(19), 4973–4991.

Gnanadesikan, A. (1999), A simple predictive model for the structure of the oceanic pycnocline, *Science*, *283*(5410), 2077–2079.

Gnanadesikan, A., R. D. Slater, P. S. Swathi, and G. K. Vallis (2005), The energetics of ocean heat transport, *J. Clim.*, *18*, 2604–2616.

Gregory, J. M. (2000), Vertical heat transports in the ocean and their effect on time-dependent climate change, *Clim. Dyn.*, *16*, 501–515.

Griffies, S. (2007), *Fundamentals of Ocean Climate Models*, 230 pp., Princeton Univ. Press, Princeton and Oxford, U. K.

Held, I. M., M. Winton, K. Takahashi, T. Delworth, F. Zeng, and G. K. Vallis (2010), Probing the fast and slow components of global warming by returning abruptly to preindustrial forcing, *J. Clim.*, *23*(9), 2418–2427.

Kostov, Y., K. C. Armour, and J. Marshall (2014), Impact of the Atlantic meridional overturning circulation on ocean heat storage and transient climate change, *Geophys. Res. Lett.*, *41*, 2108–2116, doi:10.1002/2013GL058998.

Kuhlbrodt, T., and J. M. Gregory (2012), Ocean heat uptake and its consequences for the magnitude of sea level rise and climate change, *Geophys. Res. Lett.*, *39*, L18608, doi:10.1029/2012GL052952.

Lee, S. -K., W. Park, E. van Sebille, M. O. Baringer, C. Wang, D. B. Enfield, S. G. Yeager, and B. P. Kirtman (2011), What caused the significant increase in Atlantic Ocean heat content since the mid-20th century?, *Geophys. Res. Lett.*, *38*, L17607, doi:10.1029/2011GL048856.

Marshall, D. P., and L. Zanna (2014), A conceptual model of ocean heat uptake under climate change, *J. Clim.*, *27*(22), 8444–8465.

Marshall, J., and T. Radko (2003), Residual-mean solutions for the Antarctic Circumpolar Current and its associated overturning circulation, *J. Phys. Oceanogr.*, *33*, 2341–2354.

Marshall, J., and K. Speer (2012), Closure of the meridional overturning circulation through Southern Ocean upwelling, *Nat. Geosci.*, *5*, 171–180.

McDougall, T. J. (2003), Potential enthalpy: A conservative oceanic variable for evaluating heat content and heat fluxes, *J. Phys. Oceanogr.*, *33*, 945–963.
Morrison, A., O. Saenko, A. Hogg, and P. Spence (2013), The role of vertical eddy flux in Southern Ocean heat uptake, *Geophys. Res. Lett.*, *40*, 5445–5450, doi:10.1002/2013GL057706.
Mudryk, L., P. Kushner, and C. Derksen (2013), Interpreting observed Northern Hemisphere snow trends with large ensembles of climate simulations, *Clim. Dyn.*, *43*(1-2), 345–359.
Munk, W. H. (1966), Abyssal recipes, *Deep Sea Res.*, *13*, 707–730.
Nycander, J., J. Nilsson, K. Döös, and G. Bromström (2007), Thermodynamic analysis of ocean circulation, *J. Phys. Oceanogr.*, *37*, 2038–2052.
Purkey, S. G., and G. C. Johnson (2010), Warming of global abyssal and deep Southern Ocean waters between the 1990s and 2000s: Contributions to global heat and sea level rise budgets*, *J. Clim.*, *23*(23), 6336–6351.
Saenko, O. A. (2009), On the climatic impact of wind stress, *J. Phys. Oceanogr.*, *39*(1), 89–106.
Shakespeare, C. J., and A. McC. Hogg (2012), An analytical model of the response of the meridional overturning circulation to changes in wind and buoyancy forcing, *J. Phys. Oceanogr.*, *42*(8), 1270–1287.
Solomon, S., D. Qin, M. Manning, Z. Chen, M. Marquis, K. B. Averyt, M. Tignor, and H. Miller (Eds.) (2007), *Contribution of Working Group I to the Fourth Assessment Report of the Intergovernmental Panel on Climate Change (AR4)*, Cambridge Univ. Press, New York.
Stommel, H., and A. B. Arons (1960), On the abyssal circulation of the worlds ocean—II. An idealized model of circulation pattern and amplitude in oceanic basins, *Deep Sea Res.*, *6*, 140–154.
Taylor, K. E., R. J. Stouffer, and G. A. Meehl (2012), An overview of CMIP5 and the experiment design, *Bull. Am. Meteorol. Soc.*, *93*(4), 485–498.
Toggweiler, J. R., and B. Samuels (1995), *Effect of Drake Passage on the Global Thermohaline Circulation*, vol. 42, pp. 477–500.
Weaver, A. J., et al. (2001), The UVIC Earth system climate model: Model description, climatology, and applications to past, present and future climates, *Atmosphere-Ocean*, *39*(4), 361–428.
Wolfe, C., P. Cessi, J. McClean, and M. Maltrud (2008), Vertical heat transport in eddying ocean models, *Geophys. Res. Lett.*, *35*, L23605, doi:10.1029/2008GL036138.
Wunsch, C., and P. Heimbach (2014), Bidecadal thermal changes in the abyssal ocean, *J. Phys. Oceanogr.*, *44*(8), 2013–2030.
Zhang, Y., and G. K. Vallis (2013), Ocean heat uptake in eddying and non-eddying ocean circulation models in a warming climate, *J. Phys. Oceanogr.*, *43*(10), 2211–2229.
Zika, J. D., et al. (2013a), Vertical eddy fluxes in the Southern Ocean, *J. Phys. Oceanogr.*, *43*(5), 941–955.
Zika, J. D., W. P. Sijp, and M. H. England (2013b), Vertical heat transport by the ocean circulation and the role of mechanical and haline forcing, *J. Phys. Oceanogr.*, *43*(10), 2095–2112.